ACS chemical biology

Articles

pubs.acs.org/acschemicalbiology

A WEE1 Inhibitor Analog of AZD1775 Maintains Synergy with Cisplatin and Demonstrates Reduced Single-Agent Cytotoxicity in Medulloblastoma Cells

Christopher J. Matheson,[†] Sujatha Venkataraman,[‡] Vladimir Amani,[‡] Peter S. Harris,[‡] Donald S. Backos,[†] Andrew M. Donson,[‡] Michael F. Wempe,[†] Nicholas K. Foreman,[‡] Rajeev Vibhakar,[‡] and Philip Reigan*[,†]

[†]Department of Pharmaceutical Sciences, Skaggs School of Pharmacy and Pharmaceutical Sciences, University of Colorado Anschutz Medical Campus, 12850 East Montview Boulevard, V20-2102, Aurora, Colorado 80045, United States

[‡]Department of Pediatrics and Section of Pediatric Hematology/Oncology/BMT, University of Colorado Anschutz Medical Campus, 12800 E 19th Ave, Mail Stop 8302, Aurora, Colorado 80045, United States

Supporting Information

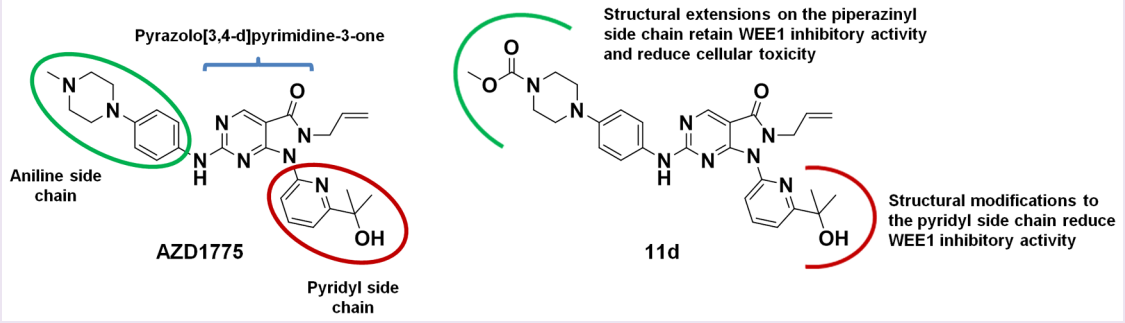

ABSTRACT: The current treatment for medulloblastoma includes surgical resection, radiation, and cytotoxic chemotherapy. Although this approach has improved survival rates, the high doses of chemotherapy required for clinical efficacy often result in lasting neurocognitive defects and other adverse events. Therefore, the development of chemosensitizing agents that allow dose reductions of cytotoxic agents, limiting their adverse effects but maintaining their clinical efficacy, would be an attractive approach to treat medulloblastoma. We previously identified WEE1 kinase as a new molecular target for medulloblastoma from an integrated genomic analysis of gene expression and a kinome-wide siRNA screen of medulloblastoma cells and tissue. In addition, we demonstrated that WEE1 prevents DNA damage-induced cell death by cisplatin and that the WEE1 inhibitor AZD1775 displays synergistic activity with cisplatin. AZD1775 was developed as a WEE1 inhibitor from an initial hit from a high-throughput screen. However, given the lack of structure−activity data for AZD1775, we developed a small series of analogs to determine the requirements for WEE1 inhibition and further examine the effects of WEE1 inhibition in medulloblastoma. Interestingly, the compounds that inhibited WEE1 in the same nanomolar range as AZD1775 had significantly reduced single-agent cytotoxicity compared with AZD1775 and displayed synergistic activity with cisplatin in medulloblastoma cells. The potent cytotoxicity of AZD1775, unrelated to WEE1 inhibition, may result in dose-limiting toxicities and exacerbate adverse effects; therefore, WEE1 inhibitors that demonstrate low cytotoxicity could be dosed at higher concentrations to chemosensitize the tumor and potentiate the effect of DNA-damaging agents such as cisplatin.

Medulloblastoma is the most common primary brain tumor in children.[1,2] The current multimodal treatment for medulloblastoma of surgical resection, posterior fossa and craniospinal irradiation, and chemotherapy has improved 5-year survival rates from 3 to >60% over the past 50 years.[3,4] Although, there has been considerable improvement in long-term survival rates, the tumor remains incurable in about a third of patients while cognitive deficits and other quality of life (QoL) measures are often impaired in long-term survivors following radiation and high-dose chemotherapy to the developing brain.[5−7] The cytotoxic agent cisplatin combined with radiation has been the cornerstone of medulloblastoma treatment for over 20 years and has produced good clinical outcomes, but these highly cytotoxic treatments are far from optimal.[8,9] There is increasing evidence that high-dose cisplatin and radiation required to circumvent tumor resistance and maintain clinical efficacy can result in lasting neurocognitive defects, stunted growth, deafness, and even secondary tumors[10−15] and that the dose and frequency of cisplatin treatment is often limited by nephrotoxicity and ototoxicity.[8,9] Therefore, there is a critical need to understand the molecular pathways in medulloblastoma to identify new molecular targets

Received: September 9, 2015
Accepted: December 22, 2015

 © XXXX American Chemical Society

DOI: 10.1021/acschembio.5b00725
ACS Chem. Biol. XXXX, XXX, XXX−XXX

that may lead to strategies to chemosensitize the tumor to safely allow dose reductions of cisplatin while maintaining clinical efficacy and resulting in improved survival and QoL outcomes.

In order to identify novel molecular targets for medulloblastoma therapy, we performed an integrated genomic screen using pathway analysis of gene expression from 16 medulloblastoma patient samples and a kinome-wide siRNA screen of medulloblastoma cells.[16] This combined analysis identified cell cycle-related kinases in the G2 checkpoint, implicating the G2 checkpoint control as a target for medulloblastoma therapy. Many cancers possess a deficient G1 checkpoint that impairs the ability of the cell to halt the cell cycle in order to repair DNA damage prior to replication.[17] This gives cancer cells a means to accumulate mutations and propagate irregularities that are favorable to cancer formation. Therefore, cancer cells are reliant on the G2 checkpoint to prevent excessive DNA damage that leads to apoptosis via mitotic catastrophe.[17,18] In normal cells, the G1 checkpoint is not compromised; therefore, the G2 checkpoint is not burdened with halting the cell cycle prior to DNA damage repair. This supports that abrogation of the G2 checkpoint will selectively impact tumorigenesis rather than normal cell growth. From our genomic analysis, we identified WEE1 as a focal kinase in two signaling pathways, and we hypothesized that targeting this kinase for inhibition could potentially disrupt multiple tumor survival mechanisms.[16] WEE1 is a tyrosine kinase that is a critical component of the ATR-mediated G2 cell cycle checkpoint control that prevents entry into mitosis in response to cellular DNA damage.[19] ATR phosphorylates and activates CHK1, which in turn activates WEE1, leading to the selective phosphorylation of cyclin-dependent kinase 1 (CDK1) at Tyr15, thereby stabilizing the CDK1-cyclin B complex and halting cell-cycle progression.[20,21] This process confers a survival advantage by allowing tumor cells time to repair damaged DNA prior to entering mitosis.[22−24] Inhibition of WEE1 abrogates the G2 checkpoint, promoting cancer cells with DNA damage to enter into unscheduled mitosis and undergo cell death via mitotic catastrophe.[25−31] Therefore, WEE1 inhibition has the potential to sensitize tumors to DNA-damaging agents, such as cisplatin.

In our previous work, we have shown that WEE1 inhibition by the small molecule inhibitor AZD1775 (previously known as MK1775) suppressed cell growth, induced apoptosis, and decreased tumor growth in medulloblastoma.[16] There are limited structure−activity relationship (SAR) data for AZD1775. It was developed as a WEE1 inhibitor by Banyu Pharmaceutical Co. from an initial hit discovered from a high-throughput screen (HTS), and it is known to have nanomolar activity with at least eight other kinases.[26] Therefore, in the present study, we have developed a small series of AZD1775 analogs by substituting the side chains around the pyrazolopyrimidinone of AZD1775 to establish a SAR for WEE1 inhibition and further examine the effects of WEE1 inhibition in medulloblastoma. Interestingly, our AZD1775 analogs that inhibited WEE1 in the same nanomolar range as AZD1775 did not exhibit the same potent inhibitory effect on medulloblastoma cell growth as single agents, yet these compounds demonstrated synergy with cisplatin at nontoxic inhibitor concentrations. Our data support that WEE1 inhibition sensitizes medulloblastoma cells to cisplatin and indicate that the cytotoxicity of AZD1775 may be uncoupled from WEE1 inhibition. AZD1775 is currently being evaluated in clinical trials as a potentiator of DNA-damaging agents for a number of cancer types; therefore, our data could be of critical importance as the off-target toxicities of AZD1775 may limit its utility in the clinic. Therefore, WEE1 inhibitors which demonstrate low cytotoxicity could be used at higher concentrations to chemosensitize the tumor and potentiate the effect of DNA-damaging agents such as cisplatin, allowing for dose reductions of DNA-damaging agents and limiting therapy-related adverse effects.

RESULTS AND DISCUSSION

Targeting WEE1 in Medulloblastoma. There is a critical need to develop new therapeutic strategies that reduce long-term adverse events that arise from chemotherapy-associated toxicities while maintaining or improving treatment efficacy in patients with medulloblastoma. We have previously identified WEE1 as a promising therapeutic target in medulloblastoma as it is a focal kinase involved in the G2 checkpoint control that prevents the accumulation of excessive DNA damage and subsequent induction of cell death.[16] Furthermore, studies have shown that strategies targeting the G2 checkpoint may be effective at inducing cancer-specific synthetic lethality while generally being well-tolerated by normal cells.[32] AZD1775 is a potent inhibitor of WEE1 kinase activity that is currently undergoing clinical trials for use in combination therapies to sensitize tumors to DNA-damaging agents. The assumption is that AZD1775, as a sensitizing agent, would be relatively nontoxic when used as a single agent; however, our results clearly demonstrate that AZD1775 negatively impacts cellular viability in medulloblastoma cells at nanomolar concentrations. Analysis of our series of AZD1775 analogs indicated that small changes in the AZD1775 structure dramatically alter WEE1 inhibitory activity or medulloblastoma cell growth inhibition independently. Our results also support that WEE1 inhibition *per se* is not responsible for the decrease in cell viability observed with AZD1775.

Structural Modification of AZD1775 and *in Vitro* Kinase Activity. Computational-based modeling of the predicted interactions of AZD1775 in the ATP-binding domain of WEE1 (Figure 1) indicated that the 4-methylpiperazinyl and pyridyl-2-propan-2-ol side chains were orientated toward the entrance of the binding cavity where a range of substitutions could be accommodated. From the model, the 4-methylpiperazinyl group can interact with Ile305, Tyr378, and Cys379 via hydrophobic and π-alkyl interactions. To understand the extent of these interactions, a series of compounds were proposed as chemical probes that retain the dialkylanilino group, while sequentially building complexity in this region with dimethylamino, piperadine, morpholine and piperazine *N*-methyl ester groups. The pyridyl-2-propan-2-ol substituent in AZD1775 was not predicted to make significant interactions with the binding pocket apart from an edge-face $\pi-\pi$ interaction with Phe433. To confirm the amenability of this group to modification, the commercially available pyridines 2-trifluoromethlpyridine and 2-methoxypyridine were identified that would retain this $\pi-\pi$ interaction, while being structurally diverse from the propan-2-ol group in AZD1775. All possible combinations of analogs (**11a−n**) and AZD1775 were synthesized (Figure 2A and Supporting Information),[33] and the IC_{50} values for each compound were determined against WEE1 in an *in vitro* recombinant kinase assay (Figure 2B, Supporting Information Figure S1). All the compounds retaining the pyridyl-2-propan-2-ol substituent (**11a−d**) of AZD1775 demonstrated potent WEE1 inhibition with AZD1775 being the most potent overall.

DOI: 10.1021/acschembio.5b00725
ACS Chem. Biol. XXXX, XXX, XXX−XXX

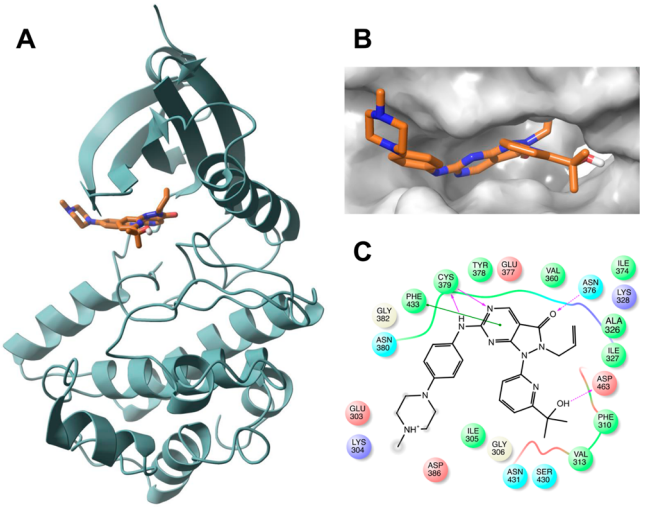

Figure 1. Molecular docking of AZD1775 in the ATP-binding site of WEE1. (A) Predicted interaction of AZD1775 (orange sticks) with WEE1 (cyano ribbon). (B) A Connolly surface applied to the ATP-binding site with AZD1775 (orange sticks). (C) A ligand interaction map for AZD1775 summarizing key interactions with the ATP-binding site of WEE1. Dashed lines indicate predicted nonbond interactions (green = $\pi-\pi$, purple = H-bond).

These data validate the computational model suggesting that the 4-methylpiperazinyl region of the molecule is solvent-exposed when bound to the kinase and is not responsible for key binding interactions beyond the dialkylanilino nitrogen. However, when the pyridine ring was modified, only compound **11m**, bearing the 2-methoxy pyridinyl substitution and retaining the 4-methylpiperazinyl group of AZD1775, demonstrated inhibitory potency comparable to AZD1775. These data indicate that, although AZD1775 is amenable to modification, small structural changes in the side chains can impact WEE1 inhibitory activity. The compounds demonstrating potent WEE1 inhibition (**11a–d**, **11m**, Supporting Information Figure S2) were selected for further evaluation with AZD1775.

Effect of WEE1 Inhibitors on Medulloblastoma Cell Growth and Viability. AZD1775 has been shown to confer significant reduction in the growth and viability of medulloblastoma cells as a single agent.[16] In order to evaluate the effect of our inhibitors under these conditions, Daoy cells were treated with AZD1775 and **11a–11n**, at 75 nM and 150 nM, and cell growth was monitored in real-time using xCELLigence analysis (ACEA Biosciences Inc.; Figure 3A, Supporting Information Figure S3). Interestingly, all compounds (**11a–11n**), including those with comparable inhibitory activity in the *in vitro* kinase assay (**11a–d**, **11m**), exhibited a reduced effect on cell growth inhibition compared with AZD1775. This difference in single agent toxicity was also observed between AZD1775 and the most potently active WEE1 inhibitors (**11d** and **11m**) by MTS assay (Figure 3B and C). Although all of the compounds tested had an effect on cell viability, it was apparent that AZD1775 (Daoy; EC_{50} = 289 ± 22 nM, ONS-76; EC_{50} = 249 ± 64 nM) had an increased single agent effect by MTS when compared to **11d** (Daoy; EC_{50} = 791 ± 95 nM, ONS-76; EC_{50} = 868 ± 94 nM) and **11m** (Daoy; EC_{50} = 558 ± 34 nM, ONS-76; EC_{50} = 760 ± 88 nM). We further compared AZD1775 with **11d** and **11m** over a concentration range in the medulloblastoma D458 suspension cell line, using flow cytometry to determine cell number and percentage viability. Cell number decreased and the percentage of nonviable cells increased compared with DMSO control at a lower concentration of AZD1775 (123.5 nM, $p < 0.01$) than **11d** (370.4 nM, $p < 0.01$) and **11m** (1.11 μM, $p < 0.001$) (Figure 4D). Although AZD1775 (IC_{50} = 18.7 ± 8 nM) exhibited greater potency than both **11d** (IC_{50} = 27.8 ± 15 nM) and **11m** (IC_{50} = 30.5 ± 8 nM) in the recombinant kinase assay, the small differences in *in vitro* IC_{50} values did not appear to account for the disparity in single agent cellular activities, particulary between AZD1775 and **11d**.

WEE1 Inhibitor Synergy with Cisplatin. An MTS assay was used to determine WEE1 inhibitor synergy with the DNA-damaging agent cisplatin, which would be an expected outcome in response to WEE1 inhibition. Daoy cells were treated for 72 h with increasing concentrations of both cisplatin and the WEE1 inhibitors (AZD1775, **11a–d**, **11m**), and the effects of drug combinations were analyzed using the Chou–Talalay equation, as previously described.[34] The Combination Index (CI) was determined for each potential drug combination. A CI value less than 1 indicates a synergistic drug combination,

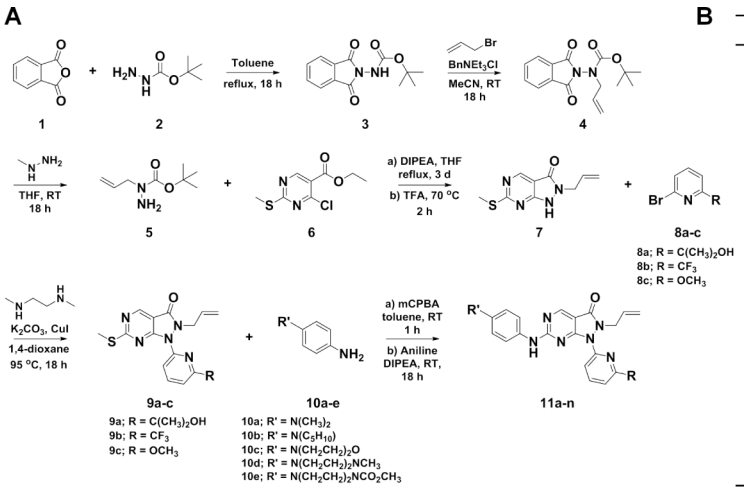

B

	R	R'	WEE1; IC_{50} (nM)
11a	$C(CH_3)_2OH$	$N(CH_3)_2$	42.8 ± 22
11b	$C(CH_3)_2OH$	$N(C_5H_{10})$	33.3 ± 20
11c	$C(CH_3)_2OH$	$N(CH_2CH_2)_2O$	37.8 ± 6
AZD1775	$C(CH_3)_2OH$	$N(CH_2CH_2)_2NCH_3$	18.7 ± 8
11d	$C(CH_3)_2OH$	$N(CH_2CH_2)_2NCO_2CH_3$	27.8 ± 15
11e	CF_3	$N(CH_3)_2$	1121 ± 236
11f	CF_3	$N(C_5H_{10})$	574 ± 340
11g	CF_3	$N(CH_2CH_2)_2O$	561 ± 300
11h	CF_3	$N(CH_2CH_2)_2NCH_3$	112 ± 24
11i	CF_3	$N(CH_2CH_2)_2NCO_2CH_3$	681 ± 93
11j	OCH_3	$N(CH_3)_2$	255 ± 11
11k	OCH_3	$N(C_5H_{10})$	147 ± 18
11l	OCH_3	$N(CH_2CH_2)_2O$	104 ± 35
11m	OCH_3	$N(CH_2CH_2)_2NCH_3$	30.5 ± 8
11n	OCH_3	$N(CH_2CH_2)_2NCO_2CH_3$	157 ± 26

Figure 2. Synthesis and inhibitory activity of novel WEE1 inhibitors. (A) Synthetic scheme for the preparation of candidate WEE1 inhibitors **11a–11n** and AZD1775. (B) Inhibitor identities and *in vitro* inhibitory activity against WEE1 kinase. IC_{50} values were determined through inhibition of recombinant WEE1 in a TR-FRET kinase assay.

DOI: 10.1021/acschembio.5b00725
ACS Chem. Biol. XXXX, XXX, XXX–XXX

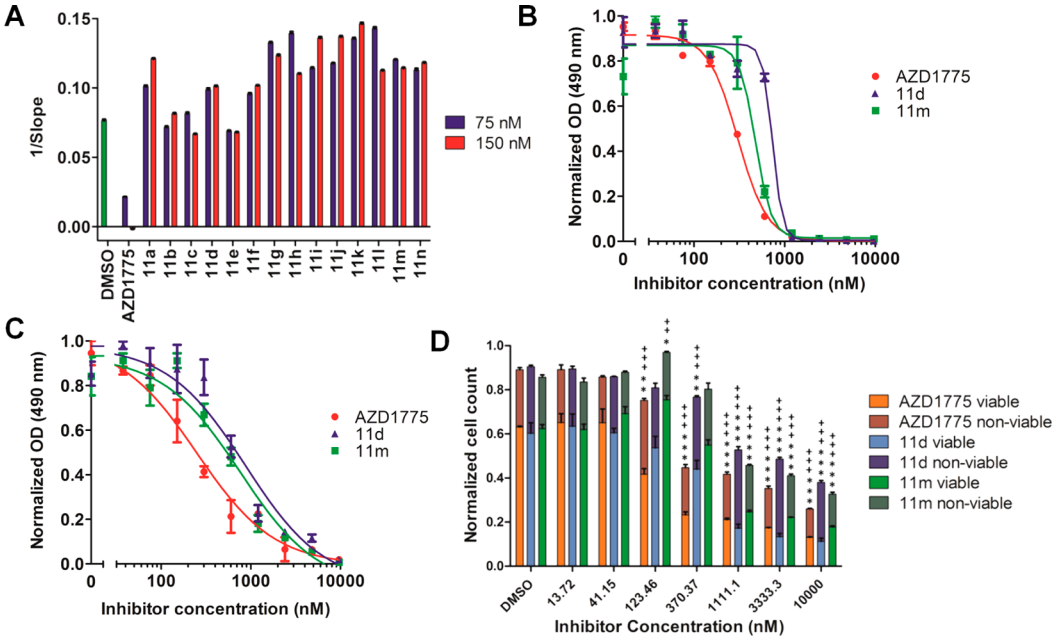

Figure 3. Single agent toxicity of AZD1775 shown to be significantly higher than the synthesized WEE1 inhibitors. (A) Daoy cell growth rate represented as 1/slope (Δcell index/h) derived from a real-time cell proliferation assay (xCELLigence) between 4 and 56 h following treatment with 75 nM (blue) and 150 nM (red) WEE1 inhibitors, compared with DMSO (green). All values have $p < 0.001$ when compared with DMSO ($n = 3$, error bars = SEM). (B) Dose−response by MTS assay for Daoy cells treated with AZD1775 (red) and the potent compounds **11d** (blue) and **11m** (green) for 72 h. AZD1775 (red) decreased the cellular metabolic output of Daoy cells ($EC_{50} = 289 \pm 22$ nM) more potently than both **11d** ($EC_{50} = 791 \pm 95$ nM) and **11m** ($EC_{50} = 558 \pm 34$ nM; $n = 3$, error bars/ ± = SEM). (C) Dose−response by MTS assay for ONS-76 cells treated with AZD1775 (red) and the potent compounds **11d** (blue) and **11m** (green) for 72 h. AZD1775 (red) decreased the cellular metabolic output of Daoy cells ($EC_{50} = 249 \pm 64$ nM) more potently than both **11d** ($EC_{50} = 868 \pm 94$ nM) and **11m** ($EC_{50} = 760 \pm 88$ nM; $n = 3$, error bars/ ± = SEM). (D) D458 cell viability and total cell number determined by flow cytometry (Viacount) when exposed to increasing concentrations of AZD1775 (orange), **11d** (blue), and **11m** (green) for 72 h ($n = 3$, error bars = SEM, compared with DMSO; total cell number; $p < 0.05$ = *, $p < 0.01$ = **, $p < 0.001$ = ***. Nonviable cell number; $p < 0.05$ = +, $p < 0.01$ = ++, $p < 0.001$ = +++).

whereas a CI of greater than 1 indicates a nonsynergistic effect. As expected, AZD1775 showed strong synergy with cisplatin across all concentrations except the lowest cisplatin and WEE1 inhibitor concentrations (Figure 4A and B). All of our WEE1 inhibitors (**11a−d**, **11m**) exhibited synergy with cisplatin to some degree, especially at higher concentrations of cisplatin. For compounds **11a−c**, the degree of synergy was reduced with respect to AZD1775 as this was only observed at the highest concentrations of cisplatin. In contrast, the more potent WEE1 inhibitors **11d** and **11m** exhibited synergistic activity at lower cisplatin concentrations and were more comparable with AZD1775. In particular, at 600 nM cisplatin, synergy was observed across all concentrations of **11d** and all but the lowest concentration of **11m**, indicating an improvement over the synergy profile of AZD1775. Dose−response curves from the MTS assay were plotted for cisplatin as a single agent and when paired with a single concentration of WEE1 inhibitor (Figure 4C). A concentration of 300 nM was chosen for the WEE1 inhibitors as no effect was observed in Daoy cells treated with WEE1 inhibitor alone at this concentration in all cases except AZD1775. When compared with cisplatin treatment, cotreatment with our inhibitors potentiated the effect of cisplatin on cell viability. The effect was also potentiated in the presence of AZD1775, but this was due to the extensive loss of cellular viability in the presence of AZD1775 alone at this concentration. Interestingly, when the treatments were repeated using AZD1775, **11d** and **11m** in combination with cisplatin in p53 wild-type ONS-76 cells, similar results were observed (Supporting Information Figure S4). These data support previous studies suggesting that WEE1 inhibition acts in synergy with DNA damage independent of cellular p53 status.[16]

Cell Permeability of WEE1 Inhibitors. Despite significant structural similarities between AZD1775 and the series of analogs, and the lead compounds possessing cLogP values within acceptable limits (AZD1775; cLogP = 2.18, **11d**; cLogP = 2.35, **11m**; cLogP = 2.89), it was possible that differences in cellular permeability and retention could explain the differential effects of each WEE1 inhibitor on cell viability. Therefore, we determined cellular uptake for AZD1775, **11d**, and **11m** at varying concentrations and incubation times (Supporting Information Figure S5). Interestingly, there was little difference between cellular concentrations of AZD1775 and **11d**, while **11m** exhibited elevated levels at all concentrations and times. Given these favorable cell permeability and retention characteristics, we further analyzed the effect of inhibitor treatment on cellular WEE1 activity.

Effect of WEE1 Inhibitor Treatment on Cellular CDK1 Phosphorylation. To confirm the effect of our WEE1 inhibitors on downstream signaling, we conducted immunoblotting analysis of phospho-CDK1 (Tyr15) levels in Daoy cell lysates following treatment with the potent WEE1 inhibitors (AZD1775, **11a−d** and **11m**; Figure 5A). Excluding **11c**, all compounds were found to reduce cellular p-CDK1 in a dose-dependent manner, similar to AZD1775. For a more quantitative analysis, an ELISA assay was used to determine the relative levels of p-CDK1 (Tyr15) in Daoy cell lysates following treatment with a broader concentration range of

DOI: 10.1021/acschembio.5b00725
ACS Chem. Biol. XXXX, XXX, XXX−XXX

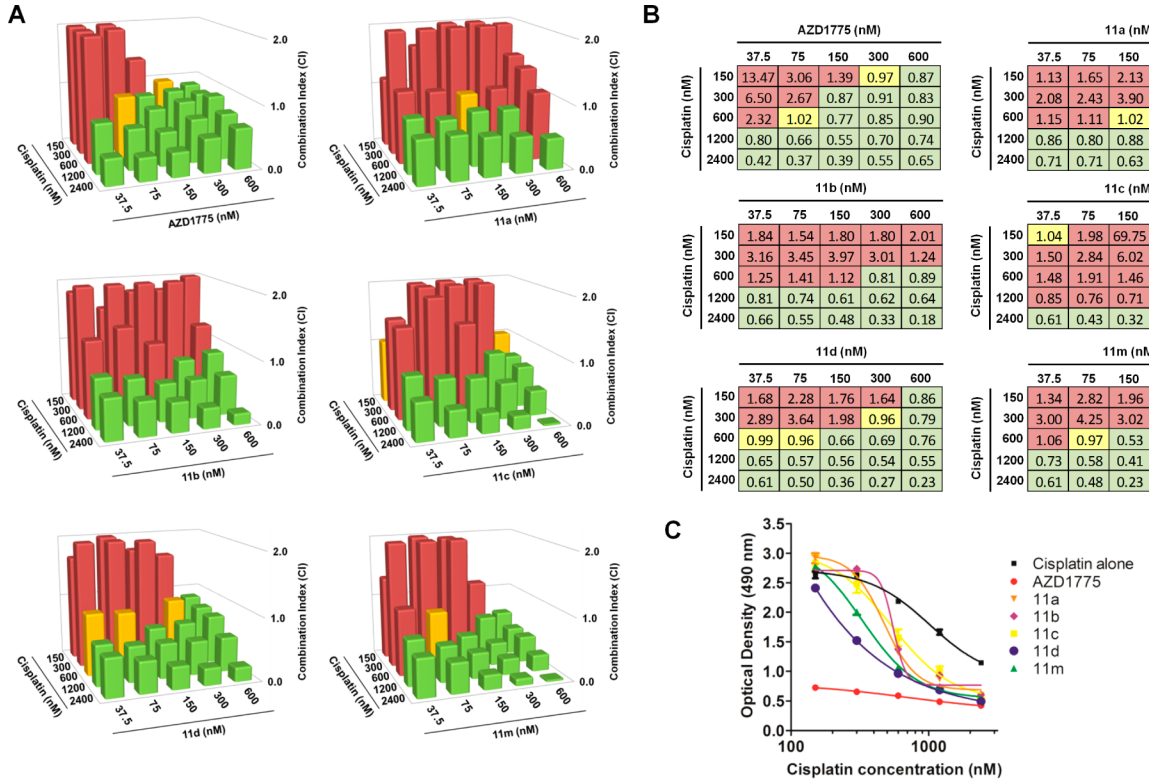

Figure 4. Identified potent inhibitors of WEE1 acting in synergy with cisplatin and potentiating the activity of cisplatin at a nontoxic concentration. (A) Combination index (CI) plots generated using an MTS assay in Daoy cells treated with WEE1 inhibitor and cisplatin combinations for 72 h (n = 3). CI values determined using the Chou−Talalay equation, with combination treatments indicated as nonsynergistic (red, ≥1.05), synergistic (green, ≤0.95), and intermediate (yellow, 0.96−1.04). (B) Numerical representation of CI plots. (C) MTS assay in Daoy cells following treatment with WEE1 inhibitors and cisplatin for 72 h. Dose−response for increasing cisplatin concentrations at a concentration (300 nM) of several WEE1 inhibitors, compared with cisplatin alone.

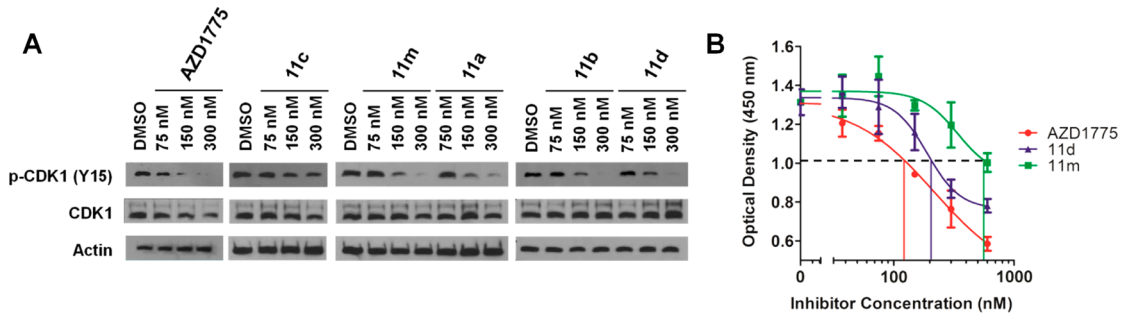

Figure 5. AZD1775 shown to decrease cellular CDK1 phosphorylation at Tyr15 at lower concentrations than potent novel WEE1 inhibitors. (A) Immunoblotting analysis of Daoy cell lysates treated with WEE1 inhibitors and DMSO control for 24 h. Membranes were probed for p-CDK1(Y15), total CDK1 and actin as a loading control. (B) Quantitative ELISA determination of relative p-CDK1 (Tyr15) levels in Daoy cell lysates (0.15 mg mL^{-1} total protein) treated with increasing concentrations of AZD1775 (red), **11d** (blue), and **11m** (green) for 24 h (n = 3, error bars = SEM). Interpolation of curves reveals that 125 nM AZD1775, 205 nM **11d**, and 565 nM **11m** are required to reduce cellular p-CDK1 (Tyr15) to the same level.

AZD1775, **11d** and **11m**, and the relative levels between samples were compared with untreated control. Cellular p-CDK1 levels were decreased to lower levels in the presence of AZD1775 versus comparable concentrations of **11d** and in particular **11m**. Interpolation of the ELISA data determined that the concentrations of **11d** and **11m** that result in the same level of cellular p-CDK1 induced by 125 nM AZD1775 treatment were 205 nM and 565 nM, respectively (Figure 5B).

Inhibition of Cellular Growth at a Fixed Level of Cellular CDK1 Phosphorylation. To evaluate the contribution of cellular p-CDK1 (Tyr15) levels, and by extension, WEE1 activity, on the observed effects of WEE1 inhibitor treatment, we repeated the real-time cell proliferation assay (xCELLigence) in Daoy cells over a broad concentration range of AZD1775 (EC_{50} = 120.6 ± 1.3 nM), **11d** (EC_{50} = 302.0 ± 0.3 nM), and **11m** (EC_{50} = 419.5 ± 1.5 nM) for 76 h (Figure 6). However, as demonstrated with ELISA determination of p-CDK1 (Tyr15) levels (Figure 5B), AZD1775 reduces the cellular activity of WEE1 at lower concentrations than both **11d** and **11m**. To determine the contribution of cellular p-CDK1 levels toward the inhibition of Daoy cell growth, the growth rate was plotted as a function of inhibitor concentration.

DOI: 10.1021/acschembio.5b00725
ACS Chem. Biol. XXXX, XXX, XXX−XXX

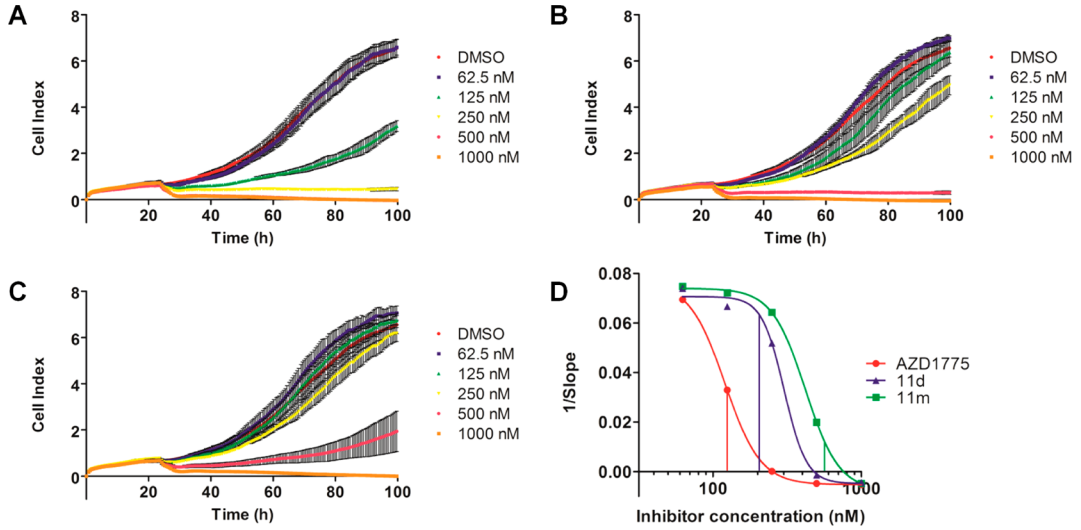

Figure 6. AZD1775 appearing to have an increased inhibitory effect on cell growth when compared with **11d** at a concentration known to result in comparable cellular WEE1 inhibition. Real-time cell proliferation plots (xCELLigence) for Daoy cells exposed to increasing concentrations of (A) AZD1775, (B) **11d** and (C) **11m**, recorded for 76 h post-treatment (drug added at 24 h; n = 3, error bars = SEM). (D) Plot for Daoy cell growth rates represented by 1/slope (Δcell index/h) for AZD1775 (red, EC_{50} = 120.6 ± 1.3 nM), **11d** (green, EC_{50} = 302.0 ± 0.3 nM), and **11m** (blue, EC_{50} = 419.5 ± 1.5 nM) across a range of inhibitor concentrations (n = 3, error bars = SEM). Growth rates were determined for the linear growth phase (t = 30−80 h). Interpolation of data reveals growth rates at fixed inhibitor concentrations; 125 nM AZD1775, 1/slope = 0.033 Δcell index/h; 205 nM **11d**, 1/slope = 0.063 Δcell index/h; 565 nM **11m**, 1/slope = 0.012 Δcell index/h.

Incubation with 125 nM AZD1775 resulted in a significantly reduced growth rate compared with vehicle control (0.033 vs 0.068; Figure 6D). In contrast, the equivalent concentration of 205 nM **11d** resulted in a nearly 2-fold increase in the rate of cell growth compared with AZD1775 (0.063 vs 0.033). For compound **11m**, the equivalent concentration of 565 nM resulted in an even greater reduction in cell growth (0.012). Taken together, these data support that WEE1 inhibition by AZD1775, **11d**, and **11m** to a fixed level of cellular CDK1 phosphorylation may be uncoupled from medulloblastoma cell growth inhibition. Therefore, the potent single agent growth inhibitory activity of AZD1775 may occur through an alternative molecular target, or a combination of WEE1 inhibition and an alternative molecular target.

AZD1775 was initially identified as a WEE1 inhibitor developed from a HTS hit; however, little is known concerning the SAR for potent WEE1 inhibition. Therefore, we designed a series of AZD1775 analogs to determine the structural requirements for WEE1 inhibition. The 2-propanol-pyridine side chain of AZD1775 was poorly amenable to structural modification as most of our attempts to modify this group resulted in a complete loss of WEE1 inhibition, with only **11m** demonstrating potent activity against WEE1, and it retained the 4-methylpiperazinyl side chain of AZD1775. However, when the 2-propanol-pyridine side chain was unaltered, it was possible to generate a series of compounds with increasing complexity in the dialkylanilino substituent of AZD1775 that retained potent WEE1 inhibition (**11a−d**). The WEE1 inhibitors (**11a−d**, **11m**, Supporting Information Figure S2) demonstrated synergy with cisplatin, with **11d** and **11m** emerging as early lead compounds. Compounds **11a−d** and **11m** at 300 nM potentiated the activity of cisplatin, but as single agents they had no observable effect in the MTS assay at this concentration. In contrast, AZD1775 significantly inhibited cell growth in Daoy cells at this concentration, and demonstrated potent single agent cytotoxicity in all medulloblastoma cell lines tested. Although the most potent inhibitors **11d** and **11m** possessed some single agent activity in the cell lines tested, the disparity in potency did not appear to be accounted for by any differences in recombinant WEE1 inhibition. AZD1775 decreased cellular p-CDK1 levels at lower concentrations than **11d** and **11m**; however, the concentrations of **11d** required to reduce p-CDK1 to a level comparable to AZD1775 treatment were not sufficient to account for the difference in single agent cytotoxicity. Taken together, our data support that the potent cytotoxicity of AZD1775 in medulloblastoma cells is uncoupled from WEE1 inhibition and that AZD1775 may interact with alternative molecular targets that result in its potent single agent cytotoxicity. In 2009, Hirai *et al.* described the small molecule MK1775 (now known as AZD1775) as a potent and selective WEE1 inhibitor, with an IC_{50} of 5.2 nmol/L in an *in vitro* kinase assay and activity against eight other kinases in a panel of 223 kinases.[26] These other kinase targets of AZD1775 included Yamaguchi sarcoma viral oncogene homologue 1 (YES1) and seven unspecified kinases that were inhibited by >80% with 1 μmol/L AZD1775. An additional study identified ABL1, LCK, LRRK2, TNK2, and SYK as targets of AZD1775 (Pubchem ID: 24856436) with K_i values below 1 μM.[35] Interstingly, microarray analysis of medulloblastoma patient tumor samples revealed that YES1, SYK, and ABL1 are all overexpressed (≥2-fold) when compared with a normal brain (Supporting Information Figure S6).

Given this narrow spectrum of activity within the kinome and rapid onset of potent cell growth inhibition from real-time cell proliferation assays (Figure 6), the alternative target(s) of AZD1775 that contribute(s) to its potent cytotoxicity may be outside the kinome. The rapid onset of decreased cell viability by AZD1775 as a single agent was our initial indicator of AZD1775 acting through alternative targets, as through WEE1 inhibition alone there would have to be a sufficient level of unrepaired DNA damage achieved through successive rounds of cell division to initiate cell death mechanisms.[36−40] In addition, we have identified **11d** as a nanomolar WEE1

DOI: 10.1021/acschembio.5b00725
ACS Chem. Biol. XXXX, XXX, XXX−XXX

inhibitor that demonstrates reduced single agent toxicity and synergy with cisplatin in medulloblastoma cells. These results indicate that the piperazinyl *N*-methyl ester of **11d** may have a reduced propensity for off-target binding and confer improved WEE1 selectivity.

In summary, we have examined a series of AZD1775 analogs and evaluated their capacity to inhibit WEE1 in an *in vitro* kinase assay, their effect on the phosphorylation of CDK1, their cytotoxicity as single agents, and their ability to potentiate the effects of cisplatin in medulloblastoma cells. We have characterized our current lead compound **11d** as a new potent selective inhibitor of WEE1 that exhibits all the desirable characteristics of a chemosensitizing agent targeting the G2 DNA-damage checkpoint including (1) reduced cytotoxic effects compared with AZD1775 within its effective concentration range as a single agent, (2) the capacity to potentiate the effect of DNA-damaging agents, such as cisplatin, and (3) favorable cell permeability and retention characteristics. In addition, our data for AZD1775 and the series of analogs support that the cytotoxicity of AZD1775 is uncoupled from WEE1 inhibition and that AZD1775 interacts with alternative molecular targets to exert its potent inhibition of cell growth. The identification of these alternative targets may be of interest for future work due to the rapid onset and pronounced cytotoxicity of AZD1775 and may also help us to understand results from clinical trials. Although clinical studies are currently at an early stage for AZD1775, it is under investigation in combination with various chemotherapeutic agents and for a number of a cancer types (16 trials logged; https://clinicaltrials.gov, accessed 09/2015). Limited clinical studies of AZD1775 as monotherapy have been performed, but they report good tolerance of AZD1775 with no dose-limiting toxicity up to 1300 mg; however, a concern is that when it is used in combination therapy, the maximum tolerated dose (MTD) of AZD1775 decreases to 200−325 mg.[41,42] In addition, the adverse events reported for AZD1775 include hematological events (myelosuppression), nausea/vomiting, and fatigue, which are common for cytotoxic agents and may be masked in combination therapies.[42] Therefore, the off-target toxicities of AZD1775 may supplement the adverse events associated with cytotoxic chemotherapy and compromise the chemosensitizing strategy of targeting WEE1 to potentiate the efficacy of DNA-damaging agents. The use of a WEE1 inhibitor, such as **11d**, that has a minimal cytotoxicity profile may maintain a high (MTD) in combination with cytotoxic chemotherapy and limit the severity of additive toxicity events. Furthermore, recent studies evaluating AZD1775 in combination with chemotherapy in brain tumors have reported that AZD1775 has limited blood brain barrier (BBB) penetration.[43] Although, it is unlikely that **11d** will have an improved BBB penetration profile over AZD1775 as their calculated blood−brain partition coefficients (qplogBB, calculated in Quikprop) are −1.8 and −0.9, respectively (where >0.3 is excellent and >−1.0 is considered poor), indicating that both AZD1775 and **11d** have little ability to cross the BBB; however, there may be scope to improve BBB penetration through examining further N-substitutions of the piperazinyl side chain. Therefore, this initial study evaluating the SAR for WEE1 inhibition provides valuable structural information for the development of inhibitors with improved BBB penetration properties to achieve optimal chemosensitizing effects in brain tumors such as medulloblastoma.

METHODS

Molecular Modeling. All computational modeling was performed using Schrödinger software (Release 2015−1: Maestro, version 10.1, Schrödinger, LLC, New York, NY, 2015). The crystal structure of the WEE1 kinase domain was downloaded from the Protein Data Bank (www.pdb.org; PDB ID 1X8B).[44] The protein structure was prepared by removing water molecules and the cocrystallized ligand; bond orders were assigned and hydrogen atoms added to the crystal structure. Finally, a restrained minimization of the protein structure was performed using the default constraint of 0.30 Å RMSD and the OPLS2.1 force field.[45] The Structure Data Format (SDF) for AZD1775 was retrieved from the PubChem database,[46] and prepared using LigPrep to assign bond orders and bond angles and then subjected to minimization using the OPLS2.1 force field.[45] Then, a Grid box was generated around the ATP-binding site of WEE1, and docking of AZD1775 was performed using Glide XP (extra precision) mode.[47]

Chemistry. AZD1775 analogs were prepared as outlined in Figure 2A and described in the Supporting Information. Briefly, *tert*-butylcarbazide (**2**) was protected through reaction with phthalic anhydride (**1**); then the carbamate nitrogen was functionalized with allyl bromide. Removal of the phthalamide protecting group with methyl hydrazine gave the key *tert*-butyl allylcarbazide (**5**), which was reacted with ethyl 4-chloro-2-methylthio-5-pyrimidinecarboxylate (**4**) in the presence of TFA to form the core pyrazollopyrimidinone scaffold (**6**). An Ullman-type aryl amination with the relevant functionalized pyridines (**8a−c**) gave the penultimate pyrazole products (**9a−c**), after which activation of the thioether with m-CPBA and reaction with anilines (**10a−e**) afforded the desired AZD1775 analogs (**11a−n**).

Recombinant Kinase Inhibition Assay. LanthaScreen Eu time-resolved fluorescence resonance energy transfer (TR-FRET) kinase binding assays (Invitrogen) were performed in 384-well, low-volume plates (Corning) using recombinant WEE1 kinase, Kinase Tracer 178 and LanthaScreen Eu-anti-GST antibody (Invitrogen). Assays were performed at 25 °C in a reaction mixture consisting of 5 μL of serially diluted inhibitor solution, 5 μL of Kinase Tracer 178 solution, and 5 μL of kinase/antibody solution. All reagents were prepared as solutions in 1× kinase buffer A (Invitrogen) at 3× final desired concentration. Inhibitor solutions were prepared such that final DMSO concentrations did not exceed 0.5%, which was shown to have no effect on kinase activity. Inhibitors were assayed in the final concentration range of 0.4 nM to 100 μM. Kinase Tracer 178 was used at a final concentration of 70 nM, and the antibody and kinase were used at final concentrations of 2 nM and 5 nM, respectively. All reagents were incubated together for 1 h at RT and read using a PerkinElmer Envision 2104 Multilabel Reader enabled for TR-FRET (excitation = 340 nm; tracer emission = 665 nm; antibody emission = 615 nm; delay = 100 μs; integration = 200 μs). Emission ratios (665 nm/615 nm) were determined for each inhibitor concentration and the data analyzed using a nonlinear regression analysis of the log dose−response curve to determine IC_{50} values.

Cell Lines and Cell Culture. Daoy, ONS-76, and D458 cells (Medulloblastoma) were obtained from ATCC and were passaged for <6 months following resuscitation. Daoy and ONS-76 cells were cultured in DMEM (Gibco) supplemented with 10% FBS (Sigma-Aldrich), 1 mM sodium pyruvate (Gibco), 1× penicillin/streptomycin solution (Cellgro), and 1× nonessential amino acids (Sigma-Aldrich) at 37 °C in an incubator humidifier with 95% air and 5% CO_2. D458 cells were cultured in DMEM (Gibco) supplemented with 10% FBS (Sigma-Aldrich), 1 mM sodium pyruvate (Gibco), 1× penicillin/streptomycin solution (Cellgro), and 1× L-glutamine (Cellgro). Seeded cells were allowed to adhere for 24 h prior to use in all assays. Under all treatment conditions, the final DMSO concentration did not exceed 0.5%.

Cellular Metabolic Viability Assay. Daoy and ONS-76 cells were seeded into sterile 96-well plates (Corning Inc.) at 2000 cells/well. Inhibitors were administered at the MTS EC_{50} of AZD1775 (Daoy; EC_{50} = 150 nM, ONS-76; EC_{50} = 290 nM) and 2-fold concentrations

DOI: 10.1021/acschembio.5b00725
ACS Chem. Biol. XXXX, XXX, XXX−XXX

above and below the EC_{50}. Cisplatin (Sigma-Aldrich) was diluted in media and was administered at the MTS EC_{50} (Daoy; EC_{50} = 600 nM, ONS-76; EC_{50} = 60 μM) and 2-fold concentrations above and below the EC_{50}. Cells were incubated for 72 h with 25 μL of each diluted drug solution. Cell viability was measured by 2 h incubation with 30 μL CellTiter 96 AQueous One Cell Proliferation reagent (Promega) and formazan concentration assessed through colorimetric analysis using a BioTek Synergy H1 plate reader (absorption = 490 nm).

Real-time Cell Proliferation Assay. Daoy cells were seeded into gold plated 96-well plates (ACEA Biosciences Inc.) at 2000 cells/well. Cells were treated with 50 μL inhibitor solutions at relevant concentrations or with equivalent DMSO vehicle at 37 °C with monitoring of cell index number at 10 min intervals for an additional 76 h. Cell index number versus time and cellular growth rate for linear growth (1/slope, Δcell index/h, t = 30−80 h) were determined for each treatment condition.

Cell Viability Determination. D458 cells were seeded into sterile 96-well round bottomed ultralow retention plates (Corning Inc.) at 5000 cells/well, and inhibitors were administered in 100 μL of media at concentrations ranging from 10 μM to 13.7 nM or equivalent DMSO control. Following incubation for 72 h, cells were pelleted and media aspirated. A total of 60 μL of TrypLE Express (Gibco) was added to each well and the plates incubated at 37 °C for 8 min followed by mechanical resuspension. A total of 50 μL of Guava Viacount reagent (EMD Millipore) was added to each well, and the plates were incubated at RT for 10 min. Wells were analyzed by flow cytometry (EMD Millipore, Guava EasyCyte Plus) with gating for viable and nonviable cell populations, and the cell concentration and percentage viability was recorded over 1000 events.

Immunoblotting Analysis. Daoy cells were plated in sterile six-well plates at 200 000 cells/well and treated with inhibitors at a final concentration of 75, 150, and 300 nM. Treated cells were incubated for 24 h, trypsinized, and resuspended in TES/SB buffer (20 mM Tris, 1 mM EDTA, 1 mM L-serine, 250 mM sucrose, 20 mM boric acid, pH 7.5) containing protease inhibitors (Roche, cOmplete). Lysates were prepared by sonication, and a total protein quantity 25 μg of each sample was loaded for SDS-PAGE. Antibodies for immunoblotting were purchased from Cell Signaling (p-CDK1 [Y15]), Abcam (CDK1), Sigma-Aldrich (β-Actin), and GE Healthcare (ECL antimouse and ECL antirabbit) and used according to recommended protocols. The chemiluminescent signal (Thermo Scientific, Super-Signal West Pico) was captured using X-ray film.

Quantification of p-CDK1 (Tyr15) Levels. Daoy cells were plated in sterile six-well plates at 200 000 cells/well and treated with inhibitors at final concentrations of 37.5, 75, 150, 300, and 600 nM and incubated for 24 h before being trypsinized and resuspended in TES/SB buffer containing protease inhibitors. Cells were lysed on ice through sonication, and cell lysates were diluted with ELISA Pathscan sample diluent to a final volume of 100 μL and protein concentration of 0.15 mg mL^{-1} prior to use. The relative concentration of p-CDK1 Tyr15 was determined using an enzyme-linked immunosorbent assay according to the recommended protocol (Cell Signaling, ELISA Pathscan phosphor-Cdc2 (Tyr15)).

Cellular Permeability of WEE1 Inhibitors. Daoy cells were plated in sterile 24-well plates at 40 000 cells/well and treated with inhibitors at a final concentration of 0.1, 0.5, 1.0, and 3.0 μM for 5, 15, 30, and 60 min prior to media aspiration. The cells were immediately washed with ice cold PBS three times, before scraping into in 500 μL of methanol/acetonitrile/water (2:2:1) containing 20 ng/mL of **11f** as an internal standard. The resultant lysate solutions were transferred into 96-deep-well plates and subjected to LC-MS/MS as follows: An Applied Biosystems Sciex 4000 (Applied Biosystems) was used; it was joined with a Shimadzu HPLC (Shimadzu Scientific Instruments, Inc.) and Leap autosampler (LEAP Technologies). Stock DMSO solutions (10.0 mM) for all compounds were prepared with (MeOH/ACN)/H_2O (4):1 and used to establish LC/MS-MS conditions. Fifteen point standard curves (0.6−900 ng/mL) were prepared for AZD1775, **11d**, and **11m**. These compounds, and the internal standard **11f**, were monitored via electrospray ionization positive ion mode (ESI+) settings: (i) ion-spray voltage 5500 V; (ii) temperature 450 °C; (iii) curtain gas (CUR; set at 10) and Collisionally Activated Dissociation (CAD gas; set at 12) were nitrogen; (iv) Ion Source, gas one (GS1) and two (GS2) were set at 30; (v) entrance potential was 10.0 V; (vi) quadruple one (Q1) and (Q3) were Low and Unit resolution, respectively; (vii) dwell time was 200 ms; and (viii) declustering potential (DP), collision energy (CE), and collision cell exit potential (CXP) are voltages (V). Compound settings were (i) AZD1775: 501.3 → 133.9 m/z, DP = 96, CE = 31, CXP = 14; (ii) **11d**: 545.4 → 527.1 m/z, DP = 96, CE = 33, CXP = 16; (iii) **11f** (internal standard): 456.2 → 415.0 m/z, DP = 81, CE = 35, CXP = 12; (iv) **11m**: 473.3 → 432.1 m/z, DP = 111, CE = 35, CXP = 14. The linear ranges (0.6−900 ng/mL) for AZD1775, **11d**, **11f**, and **11m** had correlation R^2 values of 0.9993, 0.9949, 0.9967, 0.9950, and 0.9962, respectively. These standard curves were used to determine concentration in the experimental samples. An Agilent Technologies, Zorbax extended-C18 50 × 4.6 mm column, 5 μm particle size, equipped with a C18 column guard and heated 40 °C using a flow-rate of 0.4 mL/min was used. The mobile phase consisted of (A) 10 mM ammonium acetate, 0.1% formic acid in water, and (B) 50:50 ACN/MeOH. Between samples, the autosampler was washed with a 1:1:1:1 mixture of ACN/MeOH/IPA/water containing 0.1% formic. The chromatography solvent sequence used was 95% A for 0.5 min, ramped to 95% B at 4.5 min, and held for 3.0 min; next, it was brought back to 95% A at 8.5 min and held for 0.1 min (9.0 min total run time). Samples (10 μL) were injected onto the column.

Microarray Analysis. Snap frozen medulloblastoma tumors (n = 39; WNT = 2, SHH = 10, group 3 = 11, group 4 = 15) were obtained from surgeries (Children's Hospital, Colorado), and normal brain samples (n = 34) were collected from either autopsy, epilepsy surgery, or commercial sources (COM-IRB 95-500 and 09-0906). Transcriptomic microarray analysis (Affymetrix HG-U133plus2) was performed as described previously.[48] Expression of mRNAs corresponding to known AZD1775 targets (ABL1, LCK, LRRK2, SYK, TNK2, YES1) were extracted from these microarray profiles and compared between medulloblastoma and normal brains.

Statistical Analysis. All experiments were repeated in triplicate. Statistical analyses were conducted using GraphPad Prism 5.0, and the error bars in each figure represent the standard error of the mean (SEM). Results were considered statistically significant if $p < 0.05$ by one- or two-way ANOVA as appropriate with Tukey's multiple comparison test.

■ ASSOCIATED CONTENT

Supporting Information

The Supporting Information is available free of charge on the ACS Publications website at DOI: 10.1021/acschembio.5b00725.

In vitro TR-FRET dose−response curves, chemical structures of WEE1 inhibitors, real-time cell proliferation plots in Daoy cells for compounds grouped by structure, combination index plots for WEE1 inhibitor and cisplatin treatment in ONS-76 cells, WEE1 inhibitor cell permeability and retention data, and chemical synthesis data (PDF)

■ AUTHOR INFORMATION

Corresponding Author

*Phone: 303-724-6431. Fax: 303-724-7266. E-mail: philip.reigan@ucdenver.edu.

Author Contributions

C.J.M., D.S.B., and P.R. performed computational modeling and inhibitor design. C.JM. carried out compound synthesis and *in vitro* IC_{50} determination. C.J.M., S.V., P.S.H. and V.A. performed cell testing, including synergy evaluation and single agent toxicity studies. C.J.M. and M.F.W. characterized the synthesized inhibitors and determined cellular uptake and

DOI: 10.1021/acschembio.5b00725
ACS Chem. Biol. XXXX, XXX, XXX−XXX

permeability. A.M.D. performed analysis of microarray data. C.J.M. and P.R. analyzed the data and wrote the manuscript. N.K.F., D.S.B. and R.V. analyzed data and provided review and editorial comment of the manuscript. P.R. directed the research.

Notes

The authors declare no competing financial interest.

■ ACKNOWLEDGMENTS

This study was supported by the National Institute Of Neurological Disorders And Stroke (NINDS) of the National Institutes of Health (NIH) under Award Number R21NS084084, and by the University of Colorado Computational Chemistry and Biology Core Facility and the University of Colorado Medicinal Chemistry Core Facility, which are supported in part NIH/NCATS Colorado CTSA Grant Number UL1 TR001082.

■ REFERENCES

(1) Packer, R. J., Cogen, P., Vezina, G., and Rorke, L. B. (1999) Medulloblastoma: clinical and biologic aspects. *Neuro Oncol 1*, 232−250.

(2) Pizer, B. L., and Clifford, S. C. (2009) The potential impact of tumour biology on improved clinical practice for medulloblastoma: progress towards biologically driven clinical trials. *British journal of neurosurgery 23*, 364−375.

(3) Packer, R. J. (2005) Progress and challenges in childhood brain tumors. *J. Neuro-Oncol. 75*, 239−242.

(4) O'Leary, M., Krailo, M., Anderson, J. R., and Reaman, G. H. (2008) Progress in childhood cancer: 50 years of research collaboration, a report from the Children's Oncology Group. *Semin. Oncol. 35*, 484−493.

(5) Ris, M. D., Packer, R., Goldwein, J., Jones-Wallace, D., and Boyett, J. M. (2001) Intellectual outcome after reduced-dose radiation therapy plus adjuvant chemotherapy for medulloblastoma: a Children's Cancer Group study. *J. Clin. Oncol. 19*, 3470−3476.

(6) Mulhern, R. K., Palmer, S. L., Merchant, T. E., Wallace, D., Kocak, M., Brouwers, P., Krull, K., Chintagumpala, M., Stargatt, R., Ashley, D. M., Tyc, V. L., Kun, L., Boyett, J., and Gajjar, A. (2005) Neurocognitive consequences of risk-adapted therapy for childhood medulloblastoma. *J. Clin. Oncol. 23*, 5511−5519.

(7) Packer, R. J., Cogen, P., Vezina, G., and Rorke, L. B. (1999) Medulloblastoma: clinical and biologic aspects. *Neuro-oncol 1*, 232−250.

(8) Jennings, M. T., Cmelak, A., Johnson, M. D., Moots, P. L., Pais, R., and Shyr, Y. (2004) Differential responsiveness among "high risk" pediatric brain tumors in a pilot study of dose-intensive induction chemotherapy. *Pediatr. Blood Cancer 43*, 46−54.

(9) Koberle, B., Tomicic, M. T., Usanova, S., and Kaina, B. (2010) Cisplatin resistance: preclinical findings and clinical implications. *Biochim. Biophys. Acta, Rev. Cancer 1806*, 172−182.

(10) Newton, H. B. (2001) Review of the molecular genetics and chemotherapeutic treatment of adult and paediatric medulloblastoma. *Expert Opin. Invest. Drugs 10*, 2089−2104.

(11) Onoyama, Y., Abe, M., Takahashi, M., Yabumoto, E., and Sakamoto, T. (1975) Radiation therapy of brain tumors in children. *Radiology 115*, 687−693.

(12) Knight, K. R., Kraemer, D. F., and Neuwelt, E. A. (2005) Ototoxicity in children receiving platinum chemotherapy: underestimating a commonly occurring toxicity that may influence academic and social development. *J. Clin. Oncol. 23*, 8588−8596.

(13) Paulino, A. C., Lobo, M., Teh, B. S., Okcu, M. F., South, M., Butler, E. B., Su, J., and Chintagumpala, M. (2010) Ototoxicity after intensity-modulated radiation therapy and cisplatin-based chemotherapy in children with medulloblastoma. *Int. J. Radiat. Oncol., Biol., Phys. 78*, 1445−1450.

(14) Lafay-Cousin, L., Purdy, E., Huang, A., Cushing, S. L., Papaioannou, V., Nettel-Aguirre, A., and Bouffet, E. (2013) Early cisplatin induced ototoxicity profile may predict the need for hearing support in children with medulloblastoma. *Pediatr Blood Cancer. 60*, 287.

(15) Chou, Y. T., Liao, P. W., Lin, M. C., Chou, J. C., Lin, Y. H., Lin, M. H., Tang, S. H., and Chen, M. H. (2011) Medulloblastoma presenting with pure word deafness: report of one case and review of literature. *Pediatrics and neonatology 52*, 290−293.

(16) Harris, P. S., Venkataraman, S., Alimova, I., Birks, D. K., Balakrishnan, I., Cristiano, B., Donson, A. M., Dubuc, A. M., Taylor, M. D., Foreman, N. K., Reigan, P., and Vibhakar, R. (2014) Integrated genomic analysis identifies the mitotic checkpoint kinase WEE1 as a novel therapeutic target in medulloblastoma. *Mol. Cancer 13*, 72.

(17) Chen, T., Stephens, P. A., Middleton, F. K., and Curtin, N. J. (2012) Targeting the S and G2 checkpoint to treat cancer. *Drug Discovery Today 17*, 194−202.

(18) Bucher, N., and Britten, C. D. (2008) G2 checkpoint abrogation and checkpoint kinase-1 targeting in the treatment of cancer. *Br. J. Cancer 98*, 523−528.

(19) Do, K., Doroshow, J. H., and Kummar, S. (2013) Wee1 kinase as a target for cancer therapy. *Cell Cycle 12*, 3348.

(20) Indovina, P., and Giordano, A. (2010) Targeting the checkpoint kinase WEE1: selective sensitization of cancer cells to DNA-damaging drugs. *Cancer Biol. Ther. 9*, 523−525.

(21) Jin, P., Gu, Y., and Morgan, D. O. (1996) Role of inhibitory CDC2 phosphorylation in radiation-induced G2 arrest in human cells. *J. Cell Biol. 134*, 963−970.

(22) Igarashi, M., Nagata, A., Jinno, S., Suto, K., and Okayama, H. (1991) Wee1(+)-like gene in human cells. *Nature 353*, 80−83.

(23) McGowan, C. H., and Russell, P. (1993) Human Wee1 kinase inhibits cell division by phosphorylating p34cdc2 exclusively on Tyr15. *EMBO J. 12*, 75−85.

(24) Parker, L. L., and Piwnica-Worms, H. (1992) Inactivation of the p34cdc2-cyclin B complex by the human WEE1 tyrosine kinase. *Science 257*, 1955−1957.

(25) De Witt Hamer, P. C., Mir, S. E., Noske, D., Van Noorden, C. J., and Wurdinger, T. (2011) WEE1 kinase targeting combined with DNA-damaging cancer therapy catalyzes mitotic catastrophe. *Clin. Cancer Res. 17*, 4200−4207.

(26) Hirai, H., Iwasawa, Y., Okada, M., Arai, T., Nishibata, T., Kobayashi, M., Kimura, T., Kaneko, N., Ohtani, J., Yamanaka, K., Itadani, H., Takahashi-Suzuki, I., Fukasawa, K., Oki, H., Nambu, T., Jiang, J., Sakai, T., Arakawa, H., Sakamoto, T., Sagara, T., Yoshizumi, T., Mizuarai, S., and Kotani, H. (2009) Small-molecule inhibition of Wee1 kinase by MK-1775 selectively sensitizes p53-deficient tumor cells to DNA-damaging agents. *Mol. Cancer Ther. 8*, 2992−3000.

(27) Hirai, H., Arai, T., Okada, M., Nishibata, T., Kobayashi, M., Sakai, N., Imagaki, K., Ohtani, J., Sakai, T., Yoshizumi, T., Mizuarai, S., Iwasawa, Y., and Kotani, H. (2010) MK-1775, a small molecule Wee1 inhibitor, enhances anti-tumor efficacy of various DNA-damaging agents, including 5-fluorouracil. *Cancer Biol. Ther. 9*, 514−522.

(28) Indovina, P., and Giordano, A. (2010) Targeting the checkpoint kinase WEE1: selective sensitization of cancer cells to DNA-damaging drugs. *Cancer Biol. Ther. 9*, 523−525.

(29) Leijen, S., Beijnen, J. H., and Schellens, J. H. (2010) Abrogation of the G2 checkpoint by inhibition of Wee-1 kinase results in sensitization of p53-deficient tumor cells to DNA-damaging agents. *Curr. Clin. Pharmacol. 5*, 186−191.

(30) Mir, S. E., De Witt Hamer, P. C., Krawczyk, P. M., Balaj, L., Claes, A., Niers, J. M., Van Tilborg, A. A., Zwinderman, A. H., Geerts, D., Kaspers, G. J., Peter Vandertop, W., Cloos, J., Tannous, B. A., Wesseling, P., Aten, J. A., Noske, D. P., Van Noorden, C. J., and Wurdinger, T. (2010) In silico analysis of kinase expression identifies WEE1 as a gatekeeper against mitotic catastrophe in glioblastoma. *Cancer Cell 18*, 244−257.

(31) Bridges, K. A., Hirai, H., Buser, C. A., Brooks, C., Liu, H., Buchholz, T. A., Molkentine, J. M., Mason, K. A., and Meyn, R. E. (2011) MK-1775, a novel Wee1 kinase inhibitor, radiosensitizes p53-defective human tumor cells. *Clin. Cancer Res. 17*, 5638−5648.

DOI: 10.1021/acschembio.5b00725
ACS Chem. Biol. XXXX, XXX, XXX−XXX

(32) Dillon, M. T., Good, J. S., and Harrington, K. J. (2014) Selective Targeting of the G2/M Cell Cycle Checkpoint to Improve the Therapeutic Index of Radiotherapy. *Clinical Oncology 26*, 257−265.
(33) Sakamoto, T.; Sunami, S.; Yamamoto, F.; Niiyama, K.; Bamba, M.; Takahashi, K.; Furuyama, H.; Sagara, T.; Otsuki, S.; Nishibata, T.; Yoshizumi, T.; Hirai, H. Dihydropyrazolopyrimidinone Derivatives. WO/2007/126128, 2007
(34) Donson, A. M., Weil, M. D., and Foreman, N. K. (1999) Tamoxifen radiosensitization in human glioblastoma cell lines. *J. Neurosurg. 90*, 533−536.
(35) Metz, J. T., Johnson, E. F., Soni, N. B., Merta, P. J., Kifle, L., and Hajduk, P. J. (2011) Navigating the kinome. *Nat. Chem. Biol. 7*, 200−202.
(36) Bucher, N., and Britten, C. D. (2008) G2 checkpoint abrogation and checkpoint kinase-1 targeting in the treatment of cancer. *Br. J. Cancer 98*, 523−528.
(37) Castedo, M., Perfettini, J. L., Roumier, T., Andreau, K., Medema, R., and Kroemer, G. (2004) Cell death by mitotic catastrophe: a molecular definition. *Oncogene 23*, 2825−2837.
(38) Kawabe, T. (2004) G2 checkpoint abrogators as anticancer drugs. *Mol. Cancer Ther 3*, 513−519.
(39) Vogelstein, B., Lane, D., and Levine, A. J. (2000) Surfing the p53 network. *Nature 408*, 307−310.
(40) Zhou, B. B., and Bartek, J. (2004) Targeting the checkpoint kinases: chemosensitization versus chemoprotection. *Nat. Rev. Cancer 4*, 216−225.
(41) Do, K., Wilsker, D., Ji, J., Zlott, J., Freshwater, T., Kinders, R. J., Collins, J., Chen, A. P., Doroshow, J. H., and Kummar, S. (2015) Phase I Study of Single-Agent AZD1775 (MK-1775), a Wee1 Kinase Inhibitor, in Patients With Refractory Solid Tumors. *J. Clin. Oncol. 33*, 3409.
(42) Leijen, S., Schellens, J. H., Shapiro, G., Pavlick, A. C., Tibes, R., Demuth, T., Viscusi, J., Cheng, J. D., Xu, Y., and Oza, A. M. (2010) A phase I pharmacological and pharmacodynamic study of MK-1775, a Wee1 tyrosine kinase inhibitor, in monotherapy and combination with gemcitabine, cisplatin, or carboplatin in patients with advanced solid tumors. *ASCO Meeting Abstracts 28*, 3067.
(43) Pokorny, J. L., Calligaris, D., Gupta, S. K., Iyekegbe, D. O., Jr., Mueller, D., Bakken, K. K., Carlson, B. L., Schroeder, M. A., Evans, D. L., Lou, Z., Decker, P. A., Eckel-Passow, J. E., Pucci, V., Ma, B., Shumway, S. D., Elmquist, W. F., Agar, N. Y., and Sarkaria, J. N. (2015) The Efficacy of the Wee1 Inhibitor MK-1775 Combined with Temozolomide Is Limited by Heterogeneous Distribution across the Blood-Brain Barrier in Glioblastoma. *Clin. Cancer Res. 21*, 1916−1924.
(44) Squire, C. J., Dickson, J. M., Ivanovic, I., and Baker, E. N. (2005) Structure and Inhibition of the Human Cell Cycle Checkpoint Kinase, Wee1A Kinase: An AtypicalTyrosine Kinase with a Key Role in CDK1 Regulation. *Structure 13*, 541−550.
(45) Beckstein, O., Fourrier, A., and Iorga, B. I. (2014) Prediction of hydration free energies for the SAMPL4 diverse set of compounds using molecular dynamics simulations with the OPLS-AA force field. *J. Comput.-Aided Mol. Des. 28*, 265−276.
(46) Bolton, E. E., Wang, Y., Thiessen, P. A., and Bryant, S. H. (2008) Chapter 12 - PubChem: Integrated Platform of Small Molecules and Biological Activities, in *Annual Reports in Computational Chemistry* (Ralph, A. W., and David, C. S., Eds.), pp 217−241, Elsevier.
(47) Friesner, R. A., Banks, J. L., Murphy, R. B., Halgren, T. A., Klicic, J. J., Mainz, D. T., Repasky, M. P., Knoll, E. H., Shelley, M., Perry, J. K., Shaw, D. E., Francis, P., and Shenkin, P. S. (2004) Glide: a new approach for rapid, accurate docking and scoring. 1. Method and assessment of docking accuracy. *J. Med. Chem. 47*, 1739−1749.
(48) Griesinger, A. M., Birks, D. K., Donson, A. M., Amani, V., Hoffman, L. M., Waziri, A., Wang, M., Handler, M. H., and Foreman, N. K. (2013) Characterization of Distinct Immunophenotypes across Pediatric Brain Tumor Types. *J. Immunol. 191*, 4880−4888.

DOI: 10.1021/acschembio.5b00725
ACS Chem. Biol. XXXX, XXX, XXX−XXX